1,3,4-Oxadiazole-functionalized α -amino-phosphonates as ligands for the ruthenium-catalyzed reduction of ketones

Shaima Hkiri, Christophe Gourlaouen, Soufiane Touil, Ali Samarat, David Séméril

ARTICLE

1,3,4-oxadiazole-functionalized α-aminophosphonates as ligands for the ruthenium-catalyzed reduction of ketones

Received 00th January 20xx,
Accepted 00th January 20xx

DOI: 10.1039/x0xx00000x

Shaima Hkiri,[a,b] Christophe Gourlaouen,[c] Soufiane Touil,[b] Ali Samarat,[b] David Sémeril*[a]

Three α-aminophosphonates, namely diethyl[(5-phenyl-1,3,4-oxadiazol-2-ylamino)(4-trifluoromethylphenyl) methyl]phosphonate (**3a**), diethyl[(5-phenyl-1,3,4-oxadiazol-2-ylamino)(2-methoxyphenyl)methyl]phosphonate (**3b**) and diethyl[(5-phenyl-1,3,4-oxadiazol-2-ylamino)(4-nitrophenyl)methyl]phosphonate (**3c**), were synthetized *via* the Pudovik-type reaction between diethyl phosphite and imines, obtained from 5-phenyl-1,2,4-oxadiazol-2-amine and aromatic aldehydes, under microwave irradiation. Compounds **3a-c** underwent complexation with ruthenium(II) precursor, selectively at the more basic nitrogen atom of the oxadiazole ring, leading to the corresponding ruthenium complexes **4a-c** of formula [$RuCl_2$(**L**)(*p*-cymene)] (**L** = α-aminophosphonates **3a-c**). Complexes **4a-c** proved to be efficient catalysts for the transfer hydrogenation of ketones to alcohols. All new compounds were fully characterised by elemental analysis, infrared, mass and NMR spectroscopy. An X-ray structure of the α-aminophosphonate **3b** was obtained and revealed the presence, in the solid state, of an infinite chain of **3b** units supramolecularly interlinked. Two X-ray diffraction studies carried out on ruthenium complexes confirm the specific coordination of the electron-enricher nitrogen atom of the oxadiazole ring.

Introduction

α-Aminophosphonates, which are structural analogues of natural α-amino acids, have elicited considerable interest of chemists due to their wide-range of useful properties. In addition to their well-known biological activities,[1] these phosphorus compounds have gradually developed from a synthetic challenge to a directed and rational design of novel molecular ligands with outstanding metal-complexing properties. For instance, many α-aminophosphonate ligands bearing nitrogenated heterocyclic donor atom, *i.e.* α-aminophosphonate derivatives of pyridine,[2] piperazine,[2a] quinoline[3] and imidazole[4] have demonstrated good abilities for their coordination to transition metals.

Oxadiazole derivatives, especially the 1,3,4-oxadiazole isomer, have wide pharmacological applications[5] and coordination properties.[6] Although the 1,3,4-oxadiazole moiety is present in many ruthenium complexes,[7] there are only a few examples in which the 1,3,4-oxadiazole ring is directly coordinated to the ruthenium atom.[8]

In the present investigation, we describe the synthesis and characterization of three α-aminophosphonates (**L**) incorporating a 1,3,4-oxadiazole ring, which could coordinated, *via* their electron-enriched nitrogen atom, to a ruthenium(II) precursor. The resulting ruthenium complexes of the general formula [$RuCl_2$(**L**)(η^6-*p*-cymene)] (Figure 1) could be applied as catalysts for the reduction of ketones into alcohols using the transfer hydrogenation strategy, which is a selective, efficient, safe and compatible with green chemistry principles.[9]

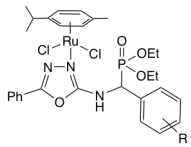

Figure 1: Targeted [$RuCl_2$(**L**)(η^6-*p*-cymene)]complexes.

Results and discussion

Preparation of α-aminophosphonates

The synthesis of ruthenium complexes **4a-c** required, firstly, the preparation of the α-aminophosphonates ligands **3a-c**, respectively (Scheme 1). Precursor **1**, which was conveniently prepared according to a method earlier reported,[10] was condensed with three aromatic aldehydes, namely 4-trifluoromethylbenzaldehyde, 2-methoxybenzaldehyde and 4-nitrobenzaldehyde in order to obtain the corresponding imines **2a-c** in 87-93 % yields. The Pudovik-type reaction[11] of these imines intermediates with diethyl phosphite under microwave irradiation[12] in neat condition (115°C and 300 W) for 10 min led to the formation of the desired α-aminophosphonates **3a-c** in 76-93 % yields. The advantages of the procedure are short reaction time, high yields, and simple work up. The structures of 1,3,4-oxadiazole derivatives **3a-c** were firmly

[a] University of Strasbourg, Synthèse Organométallique et Catalyse, UMR-CNRS 7177, 4 rue Blaise Pascal, 67008 Strasbourg, France; E-mail: dsemeril@unistra.fr
[b] University of Carthage, Faculty of Sciences of Bizerte, LR18ES11, Laboratory of Hetero-Organic Compounds and Nanostructured Materials, 7021, Bizerte, Tunisia
[c] University of Strasbourg, Laboratoire de Chimie Quantique, UMR-CNRS 7177, 4 rue Blaise Pascal, 67008 Strasbourg, France

† "Dedicated to Prof Christian Bruneau for his outstanding contribution to catalysis"

Electronic Supplementary Information (ESI) available: computational details and characteristic data for the compounds reported in this article. See DOI: 10.1039/x0xx00000x

established by well-defined infrared, multi-nucleus NMR spectroscopy (^{1}H, ^{13}C, ^{31}P and ^{19}F), mass spectrometry and elemental analysis (see the experimental section). Their ^{31}P{^{1}H} NMR spectra in DMSO-d_6 show a quadruplet at 19.4 ppm for **3a**, due to phosphorus/fluorine coupling ($^{7}J_{PF}$ = 2.2 Hz), and singlets at 20.7 and 18.8 ppm, for **3b** and **3c**, respectively. The ^{1}H NMR spectra revealed for the NH signals (δ = 8.87-9.18 ppm) a doublet of doublets due to a proton/proton ($^{3}J_{HH}$ = 6.0-10.2 Hz) and a phosphorus/proton ($^{3}J_{PH}$ = 1.5-3.9 Hz) vicinal couplings. The mass spectra analysis display peaks at 456.13, 418.15 and 433.13, for **3a**, **3b** and **3c**, respectively, corresponding to their $[M + H]^{+}$ cations with the expected isotopic profiles.

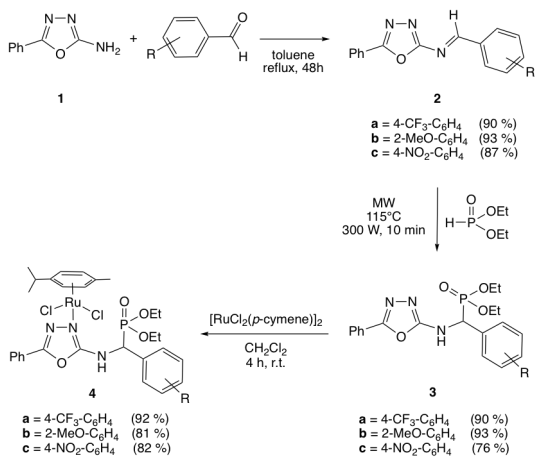

Scheme 1: Synthesis of α-aminophosphonates **3a-c** and the corresponding ruthenium complexes **4a-c**.

The α-aminophosphonate **3b** crystallises in the triclinic asymmetric space group *P* -1 with two distinct enantiomeric molecules (A and B molecules in which C9 and B C29 have a *R* and a *S* configuration, respectively; Figure 2). The oxadiazole and phenyl aromatic rings are almost planar with dihedral angles of 1.27° in B and 4.47° in A. The study revealed the presence in the solid state of an infinite chain of **3b** units supramolecularly interlinked. A (*R*)- and a (*S*)-molecule of **3b** dimerise *via* hydrogen bonds between their N-H and P=O moieties (H•••O 2.007 Å)[13] to form a racemic dimer, which in turn self-organises *via* π-π interactions between the oxadiazole and the phenyl rings (O-phenyl centroid 3.369 Å and between the centroid of oxadiazole and centroid of phenyl 3.621 Å)[14] (Figure 3).

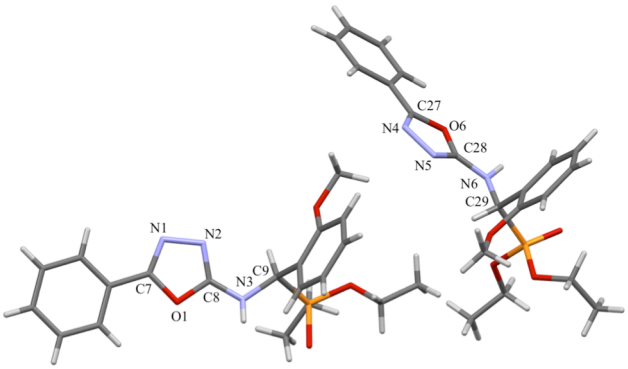

Figure 2: X-ray crystallographic structure of **3b** showing the two enantiomers. Important bond lengths (Å) and angles (°): N1-N2 1.419(5), N2-C8 1.304(5), C8-O1 1.365(5), O1-C7 1.385(5), C7-N1 1.275(6), C8-N3 1.341(5), N4-N5 1.419(5), N5-C28 1.297(5), C28-O6 1.365(5), O6-C27 1.384(5), C27-N4 1.281(6), C28-N6 1.347(5), C7-N1-N2 107.1(3), N1-N2-C8 104.9(3), N2-C8-O1 113.6(3), C8-O1-C7 101.5(3), O1-C7-N1 112.9(3), C27-N4-N5 106.9(3), N4-N5-C28 105.0(3), N5-C28-O6 113.8(4), C28-O6-C27 101.5(3), O6-C27-N4 112.7(4).

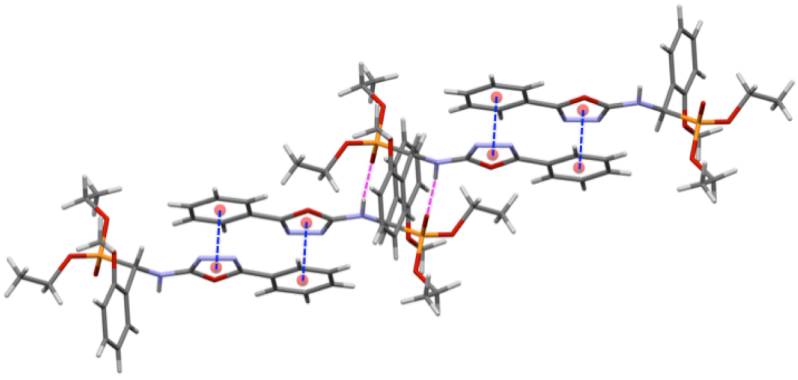

Figure 3: Self-organised structure of **3b** *via* hydrogen bonds (magenta) and π-π (bleu) interactions.

Preparation of ruthenium(II) complexes

The natural bond orbital charge analysis carried on **3a** (*see Supporting Information*) reveals that the presence of the amine moieties polarises the oxadiazole ring. If the nitrogen at position 4 in the oxadiazole ring (N1 in Figure 2) is slightly affected, there is a strong polarisation of the nitrogen at position 3 in the oxadiazole ring (N2 in Figure 2), which becomes more basic. Consequently, the latter nitrogen atom should be preferentially coordinated to a metal cation.

The α-aminophosphonates **3a-c** readily formed complexes with ruthenium(II) precursor. Thus by using a Ru/L stoichiometry of 1:1, the reaction of **3a-c** with $[RuCl_2(p\text{-cymene})]_2$ in CH_2Cl_2 at room temperature for 4 h led to the formation of complexes **4a-c** in 81-92 % yields (Scheme 1). The ^{31}P NMR spectra of the obtained complexes display a slight upfield shift (around 3.5 ppm) with regard to the free α-aminophosphonates. Infrared measurements show that the band at ~1600 cm^{-1} for free ligands (ν(C=N) stretching vibrations of the oxadiazole ring) shifts towards higher wave numbers by 40-50 cm^{-1} in the complexes, which confirms the coordination of a nitrogen atom to the metal centre. The mass spectra analysis, which show peaks corresponding to $[M - Cl]^{+}$, $[M + Na]^{+}$ and $[M + K]^{+}$ cations with the expected isotopic profiles, unambiguously confirm the coordination of the α-aminophosphonates to the ruthenium precursor. The formation of the complexes

coordinated by the nitrogen in position 3 of the oxadiazole ring (noted N1 in the X-ray structures; Figure 4 and Figure 6) was confirmed by a single X-ray diffraction studies. The complexes crystallise in the monoclinic form with the $P2_1/n$ space group. Four molecules of complexes are present in the racemic unit cell, two ruthenium atoms are coordinated to a (*S*)-α-aminophosphonate and the two others to a (*R*)-α-aminophosphonate. The ruthenium atom has a typical pseudooctahedral geometry with the *p*-cymene occupying three adjacent sites of the octahedron (Ru-centroid of *p*-cymene = 1.663 and 1.656 Å in complexes **4a** and **4b**, respectively).[15] The three others sites are occupied with two chloride atoms and the α-aminophosphonate coodinated by its oxadiazole ring, which is almost orthogonal to the coordinated *p*-cymene (dihedral angle of 80.51 and 86.29° in complexes **4a** and **4b**, respectively). The bond lengths of Ru-Cl and Ru-N were found to be 2.432, 2.432 and 2.137 Å, respectively in complex **4a** and 2.429, 2.433 and 2.125 Å, respectively in complex **4b**. In the solid state, complex **4b** formation of dimers was observed, formed from a (*R*)- and a (*S*)-**3b**. The two complexes were supramolecularly linked *via* four hydrogen bonds between aromatic CH of *p*-cymene and chloride atoms (CH•••Cl 2.757 and 2.806 and Å; Figure 7). The most striking feature is the presence of a hydrogen bond involving a chlorine atom and the NH (length NH•••Cl 2.280 and 2.371 Å in complexes **4a** and **4b**, respectively). The presence of a strong NH•••Cl hydrogen bond was confirmed by the noncovalent interaction (NCI) analysis of the density functional theory (DFT)-optimised structure carried out on the ruthenium complex **4a** (Figure 5). Furthermore, the calculations reveal that coordination of by the oxadiazole ring by its nitrogen in position 3 (noted N1 in the X-ray structures) is favour due to higher basicity of this nitrogen atom, lower steric constraints and the presence of the NH•••Cl hydrogen bond (*see Supporting Information*).

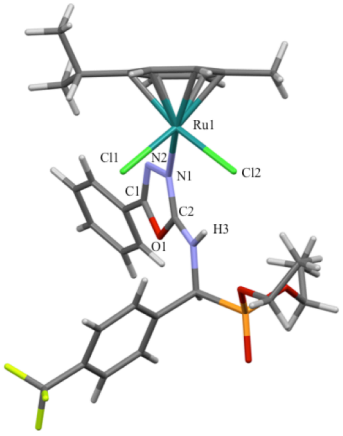

Figure 4: X-ray crystallographic structure of ruthenium complex **4a**. For clarity raison, only one of the four molecule presents in the unit cell is shown. Important bond lengths (Å) and angles (°): Ru1-Cl1 2.4320(5), Ru1-Cl2 2.4322(5), Ru1-N1 2.1369(15), N1-N2 1.413(2), N2-C1 1.283(2), C1-O1 1.381(2), O1-C2 1.355(2), C2-N1 1.213(2), Cl1-Ru1-N1 83.99(4), Cl1-Ru1-Cl2 87.88(2), Cl2-Ru1-N1 89.45(4) C1-N2-N1 106.25(14), N2-N1-C2 106.29(14), N1-C2-O1 111.92(15), C2-O1-C1 102.97(14), O1-C1-N2 112.58(15).

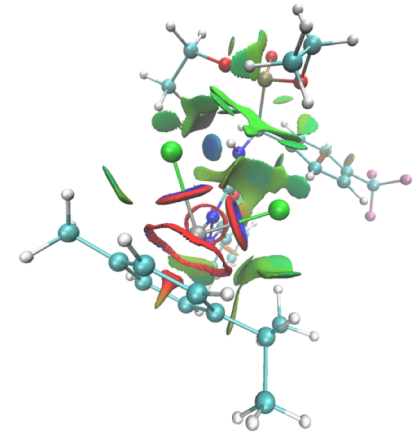

Figure 5: Visualising the noncovalent interactions in complex **4a** with attractive electrostatic interactions in blue, attractive dispersion forces in green and steric repulsions in red.

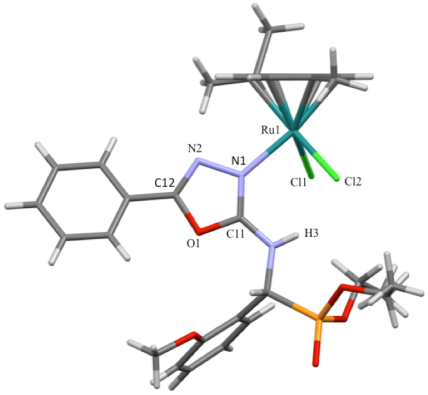

Figure 6: X-ray crystallographic structure of ruthenium complex **4b**. For clarity raison, only one of the four molecule presents in the unit cell is shown. Important bond lengths (Å) and angles (°): Ru1-Cl1 2.4330(7), Ru1-Cl2 2.4293(7), Ru1-N1 2.125(2), N1-N2 1.410(3), N2-C12 1.282(4), C12-O1 1.376(4), O1-C11 1.350(3), C11-N1 1.315(4), Cl1-Ru1-N1 84.03(7), Cl1-Ru1-Cl2 89.54(3), Cl2-Ru1-N1 87.21(7) C12-N2-N1 105.9(3), N2-N1-C11 106.5(2), N1-C11-O1 111.7(3), C11-O1-C12 103.0(2), O1-C12-N2 112.9(3).

Reduction of ketones

The ruthenium complexes **4a-c** were evaluated as catalysts for reduction of ketones. The corresponding tests were performed in the presence of a base in *iso*-propyl alcohol (^{i}PrOH) (Scheme 2).

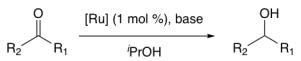

Scheme 2: Ruthenium-catalysed reduction of ketones.

In order to determine the optimum catalytic conditions, ruthenium complex **4a** (1 mol %) was used as model catalyst in the reduction of acetophenone in ^{i}PrOH as solvent. The reaction

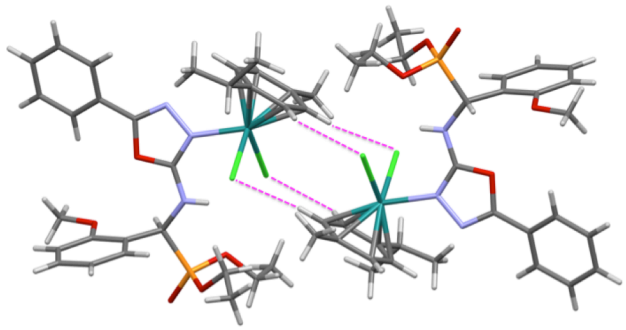

Figure 7: Self-organised structure of **4b** *via* hydrogen bonds (magenta) interactions.

was studied with various bases under different conditions. Initially, the reaction was performed with of K_3PO_4 as base at 80°C for 2 h. Thus, a conversion of 67 % was measured based on ^{1}H NMR analysis (Table 1, entry 1). As control experiments, no products were observed without the addition of ruthenium complex **4a** or base. In the first series of tests, we determined the optimal base by employing NaOEt, NaOAc, KOAc, Cs_2CO_3, K_2CO_3, KOH or NaOH. As can be inferred from the results (Table 1, entries 2-8), the most efficient base was NaOH, which led to a conversion of 95 % (Table 1, entry 8). Operating at lower temperature (60°C) led to a lower conversion (17 %; Table 1, entry 9). In contrast, carrying out the reaction at 100°C increased the catalysis, and a full conversion was observed in only one hour (Table 1, entry 10). Substitution of the CF_3 moiety by a NO_2 function on the ruthenium complex, use of precatalyst **4b**, drastically reduced the formation of alcohol (conversion of 38 %; Table 1, entry 14). Interestingly, carrying out the catalysis with a bulkier aromatic substituent on the ruthenium, complex **4c**, slightly reduced the effectiveness of the catalyst, conversions of 59 and 57 % were measured using **4a** and **4c**, respectively (Table 1, entries 13 and 15). Note that, under our catalytic conditions, tests realised in the presence of a drop of mercury,[16] no significant change in activities were observed (Table 1, entries 11 and 12), suggesting that no ruthenium nanoparticules were present.[17]

Table 1. Ruthenium-catalysed reduction of acetophenone – screening of catalytic conditions.[a]

Entry	[Ru]	Base	Time (h)	Hg	T (°C)	Conv. (%)
1	**4a**	K_3PO_4	2	no	80	67
2	**4a**	NaOEt	2	no	80	41
3	**4a**	NaOAc	2	no	80	31
4	**4a**	KOAc	2	no	80	28
5	**4a**	Cs_2CO_3	2	no	80	16
6	**4a**	K_2CO_3	2	no	80	12
7	**4a**	KOH	2	no	80	76
8	**4a**	NaOH	2	no	80	95
9	**4a**	NaOH	2	no	60	17
10	**4a**	NaOH	1	no	100	100
11	**4a**	NaOH	1	yes	80	62
12	**4a**	NaOH	1	yes	100	97
13	**4a**	NaOH	1	no	80	59
14	**4b**	NaOH	1	no	80	38
15	**4c**	NaOH	1	no	80	57

[a] Reagents and conditions: ruthenium complex (1 mol %), acetophenone (1.0 mmol), base (0.25 mmol), ^{i}PrOH (5 mL). The conversions were determined by ^{1}H NMR spectroscopy by integration of the CH_3 signals.

Applying these optimised conditions (NaOH as base at 100°C) for 2 h, the precatalyst **4a** was assigned into hydride transfer of several ketones. Seven aryl methyl ketones, namely acetophenone, 4'-chloroacetophenone, 4'-bromoacetophenone, 4'-nitroacetophenone, 4'-methoxyacetophenone, 2',4'-dichloroacetophenone and 2'-bromoacetophenone, were tested. Conversions higher than 93 % were observed in the cases of acetophenone and halogenated acetophenones. For example, conversions of 97 % and 93 % were measured for the reduction of 4'-chloroacetophenone and 2',4'-dichloroacetophenone or 2'-bromoacetophenone, respectively. The presence of a nitro or a methoxy substituent on the aromatic moiety led to low or moderated conversions, in fact, only 7 % and 66 % of 4'-nitroacetophenone and 4'-methoxyacetophenone, respectively, were reduced into the corresponding alcohol. The precatalyst **4a** was efficient to carried out the hydride transfer on dialkyl and cyclic ketones, conversion of 77 %, 61 % and 93 % were measured starting from 3,3-dimethylbutan-2-one, cyclopentanone and cyclohexanone, respectively (Figure 8).

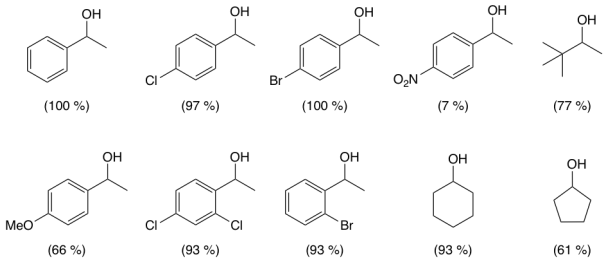

Figure 8: Formation of alcohols, reagents and conditions: ruthenium complex 4a (1 mol %), ketone (1.0 mmol), base (0.25 mmol), ^{i}PrOH (5 mL), 100°C, 2 h. The conversions were determined by ^{1}H NMR spectroscopy.

Conclusions

We have shown that the synthesis of three α-aminophosphonates, in their racemic form, incorporating a 1,3,4-oxadiazole moiety, in which the nitrogen atom closer to the amine group is electrically richer than the second one. The more basic nitrogen could easily react with a ruthenium(II) precursor leading to the formation of the corresponding [$RuCl_2$(**L**)(*p*-cymene)] (**L** = α-aminophosphonate) complexes. Two X-ray diffraction studies confirm the specific coordination of the electronic richer nitrogen atom of the oxadiazole ring. The latter ruthenium(II) complexes were assigned

in the transfer hydrogenation of ketones. Further work is aimed at exploiting the potential chirality of α-aminophosphonates and their application as ligands in the ruthenium-catalyzed asymmetric reduction of C=O and C=N bonds.

Experimental part

All manipulations involving phosphorus derivatives were carried out under dry argon. Solvents were dried by conventional methods and were distilled immediately before use. Routine ^{1}H, $^{13}C\{^{1}H\}$, $^{31}P\{^{1}H\}$ and $^{19}F\{^{1}H\}$ spectra were recorded with Bruker FT instruments (AC 300 and 500). ^{1}H NMR spectra were referenced to residual protonated solvents (δ = 2.50 ppm for DMSO-d_6 and δ = 7.26 ppm for $CDCl_3$). ^{13}C NMR chemical shifts are reported relative to deuterated solvents (δ = 39.52 ppm for DMSO-d_6 and δ = 77.16 ppm for $CDCl_3$). ^{31}P and ^{19}F NMR spectroscopic data are given relative to external H_3PO_4 and CCl_3F, respectively. Chemical shifts and coupling constants are reported in ppm and Hz, respectively. Infrared spectra were recorded with a Bruker FT-IR Alpha-P spectrometer. Microwave irradiation was carried out using the CEM Discover microwave synthesis system equipped with a pressure controller (17 bar). Elemental analyses were carried out by the Service de Microanalyse, Institut de Chimie, Université de Strasbourg. 5-Phenyl-1,3,4-oxadiazol-2-amine (**1**) was prepared by literature procedures.[10]

General procedure for the synthesis of (*E*)-1-(aryl)-*N*-(5-phenyl-1,3,4-oxadiazol-2-yl)methanimine 2a-c. In a round bottomed flask equipped with a Dean Stark apparatus, a mixture of phenyl-1,3,4-oxadiazol-2-amine (1) (2.0 mmol) and aryl aldehyde (3.0 mmol) in toluene (20 mL) was refluxed for 48 h. After cooling to room temperature, the solvent was evaporated and the crude product was washed with cool ethanol (15 mL), filtered and dried under vacuum to afford the desired imine.

(*E*)-1-(4-Trifluoromethylphenyl)-*N*-(5-phenyl-1,3,4-oxadiazol-2-yl) methanimine (2a). White solid, yield 90 %. **^{1}H NMR (300 MHz, DMSO-d_6):** δ = 9.47 (s, 1H, N=CH), 8.33 (d, 2H, arom. CH of $C_6H_4CF_3$, $^{3}J_{HH}$ = 8.4 Hz), 8.09 (dd, 2H, arom. CH of C_6H_5, $^{3}J_{HH}$ = 7.2 Hz, $^{4}J_{HH}$ = 1.8 Hz), 7.99 (d, 2H, arom. CH of $C_6H_4CF_3$, $^{3}J_{HH}$ = 8.4 Hz), 7.68-7.60 (m, 3H, arom. CH of C_6H_5) ppm; **$^{13}C\{^{1}H\}$ NMR (126 MHz, DMSO-d_6):** δ = 169.48 (s, N=CH), 166.26 (s, arom. Cquat C(N)=N), 163.57 (s, arom. Cquat C(Ph)=N), 138.29 (s, arom. Cquat of $C_6H_4CF_3$), 133.46 (q, arom. Cquat *C*CF_3, $^{2}J_{CF}$ = 31.9 Hz), 132.68 (s, arom. CH), 131.31 (s, arom. CH), 129.96 (s, arom. CH), 126.98 (s, arom. CH), 126.64 (d, arom. CH, $^{3}J_{CF}$ = 3.4 Hz), 124.25 (q, CF_3, $^{1}J_{CF}$ = 273.2 Hz), 123.88 (s, arom. Cquat of C_6H_5) ppm; **$^{19}F\{^{1}H\}$ NMR (282 MHz, DMSO-d_6):** δ = -61.61 (s, CF_3) ppm. Elemental analysis calcd. (%) for $C_{16}H_{10}ON_3F_3$ (317.27): C 60.57, H 3.18, N 13.24; found C 60.62, H 3.22, N 13.18.

(*E*)-1-(2-Methoxyphenyl)-*N*-(5-phenyl-1,3,4-oxadiazol-2-yl)methan imine (2b). White solid, yield 93 %. **^{1}H NMR (300 MHz, DMSO-d_6):** δ = 9.53 (s, 1H, N=CH), 8.12 (dd, 1H, arom. CH, $^{3}J_{HH}$ = 7.8 Hz, $^{4}J_{HH}$ = 1.5 Hz), 8.06-8.02 (m, 2H, arom. CH), 7.69 (td, 1H, arom. CH, $^{3}J_{HH}$ = 7.6 Hz, $^{4}J_{HH}$ = 1.5 Hz), 7.65-7.59 (m, 3H, arom. CH), 7.25 (d, 1H, arom. CH, $^{3}J_{HH}$ = 8.4 Hz), 7.14 (t, 1H, arom. CH, $^{3}J_{HH}$ = 7.5 Hz), 3.96 (s, 3H, OCH_3) ppm; **$^{13}C\{^{1}H\}$ NMR (126 MHz, DMSO-d_6):** δ = 166.67 (s, arom. Cquat ortho of OCH_3), 164.34 (s, N=CH), 162.75 (s, arom. Cquat C(Ph)=N), 160.96 (s, arom. Cquat C(N)=N), 136.53 (s, arom. CH), 131.95 (s, arom. CH), 129.44 (s, arom. CH), 127.63 (s, arom. CH), 126.36 (s, arom. CH), 123.59 (s, arom. Cquat), 122.10 (s, arom. Cquat), 121.11 (s, arom. CH), 112.58 (s, arom. CH), 56.13 (s, OCH_3) ppm. Elemental analysis calcd. (%) for $C_{16}H_{13}O_2N_3$ (279.29): C 68.81, H 4.69, N 15.04; found C 68.84, H 4.73, N 14.99.

(*E*)-1-(4-Nitrophenyl)-*N*-(5-phenyl-1,3,4-oxadiazol-2-yl)methan imine (2c). Yellow solid, yield 87 %. **^{1}H NMR (300 MHz, DMSO-d_6):** δ = 9.51 (s, 1H, N=CH), 8.44 (d, 2H, arom. CH of $C_6H_4NO_2$, $^{3}J_{HH}$ = 9.0 Hz), 8.37 (d, 2H, arom. CH of $C_6H_4NO_2$, $^{3}J_{HH}$ = 9.0 Hz), 8.09 (d, 2H, arom. CH of C_6H_5, $^{3}J_{HH}$ = 8.1 Hz), 7.68-7.62 (m, 3H, arom. CH of C_6H_5) ppm; **$^{13}C\{^{1}H\}$ NMR (126 MHz, DMSO-d_6):** δ = 168.44 (s, N=CH), 165.69 (s, arom. Cquat C(N)=N), 163.21 (s, arom. Cquat C(Ph)=N), 150.27 (q, arom. Cquat CNO_2), 139.60 (s, arom. Cquat of $C_6H_4NO_2$), 132.31 (s, arom. CH), 131.31 (s, arom. CH), 129.54 (s, arom. CH), 126.57 (s, arom. CH), 124.34 (s, arom. CH), 123.38 (s, arom. Cquat of C_6H_5) ppm. Elemental analysis calcd. (%) for $C_{15}H_{10}O_3N_4$ (294.27): C 61.22, H 3.43, N 19.04; found C 61.18, H 3.35, N 18.97.

General procedure for the synthesis of diethyl[(5-phenyl-1,3,4-oxadiazol-2-ylamino)(aryl)methyl]phosphonate 3a-c. In a round bottomed flask, a mixture of (*E*)-1-(aryl)-*N*-(5-phenyl-1,3,4-oxadiazol-2-yl)methanimine (**2**) (1.0 mmol) and diethyl phosphite (0.25 mL, 2.0 mmol) was added and irradiated under microwave in neat condition at 115°C for 10 min at 300 W. After cooling to room temperature, the crude product was washed with EtO_2 (3 x 10 mL), filtered and dried under vacuum to afford a white solid. In the case of **3c**, the crude product was purified by column chromatography (EtOAc/Et_2O, 50:50, v/v) to afford a white solid.

Diethyl[(5-phenyl-1,3,4-oxadiazol-2-ylamino)(4-trifluoromethyl-phenyl)methyl]phosphonate (3a). Yield 90 %. **^{1}H NMR (300 MHz, DMSO-d_6):** δ = 9.14 (dd, 1H, NH, $^{3}J_{HH}$ = 6.0 Hz, $^{3}J_{PH}$ = 1.5 Hz), 7.85-7.77 (m, 6H, arom. CH), 7.56-7.51 (m, 3H, arom. CH), 5.38 (dd, 1H, CHP, $^{2}J_{PH}$ = 13.5 Hz, $^{3}J_{HH}$ = 5.7 Hz), 4.08-3.88 (m, 4H, OCH_2CH_3), 1.18 (t, 3H, OCH_2CH_3, $^{3}J_{HH}$ = 4.2 Hz), 1.10 (t, 3H, OCH_2CH_3, $^{3}J_{HH}$ = 4.2 Hz) ppm; **$^{13}C\{^{1}H\}$ NMR (126 MHz, DMSO-d_6):** δ = 162.95 (d, arom. Cquat para of CF_3, $^{2}J_{CP}$ = 11.2 Hz), 158.41 (s, arom. Cquat C(Ph)=N), 140.37 (s, arom. Cquat C(NH)=N), 130.80 (s, arom. CH), 129.30 (s, arom. CH), 128.92 (d, arom. CH, $^{3}J_{CP}$ = 4.6 Hz), 128.43 (q, arom. Cquat *C*CF_3, $^{2}J_{CF}$ = 32.8 Hz), 125.30 (s, arom. CH), 125.14 (s, arom. CH), 124.20 (q, CF_3, $^{1}J_{CF}$ = 272.5 Hz), 123.94 (s, arom. Cquat of C_6H_5), 62.91 (d, OCH_2CH_3, $^{2}J_{CP}$ = 23.1 Hz), 62.86 (d, OCH_2CH_3, $^{2}J_{CP}$ = 22.9 Hz), 54.10 (d, CHP, $^{1}J_{CP}$ = 153.3 Hz), 16.16 (d, OCH_2CH_3, $^{3}J_{CP}$ = 19.1 Hz), 16.12 (d, OCH_2CH_3, $^{3}J_{CP}$ = 19.3 Hz) ppm; **$^{31}P\{^{1}H\}$ NMR (121 MHz, DMSO-d_6):** δ = 19.4 (q, P(O), $^{7}J_{PF}$ = 2.2 Hz) ppm; **$^{19}F\{^{1}H\}$ NMR (282 MHz, DMSO-d_6):** δ = -60.97 (d, CF_3, $^{7}J_{PF}$ = 2.0 Hz) ppm. IR: ν = 1600 cm^{-1} (C=N). MS (ESI-TOF): m/z = 456.13 $[M + H]^+$, 478.11 $[M + Na]^+$, 494.09 $[M + K]^+$ (expected isotopic profiles). Elemental analysis calcd. (%) for $C_{20}H_{21}O_4N_3F_3P$ (455.37): C 52.75, H 4.65, N 9.23; found C 52.71, H 4.59, N 9.20.

Diethyl[(5-phenyl-1,3,4-oxadiazol-2-ylamino)(2-methoxyphenyl) methyl]phosphonate (3b). Yield 93 %. **^{1}H NMR (300 MHz, DMSO-d_6):** δ = 8.87 (dd, 1H, NH, $^{3}J_{HH}$ = 10.2 Hz, $^{3}J_{PH}$ = 2.7 Hz), 7.81-7.78 (m, 2H, arom. CH), 7.62 (dt, 1H, arom. CH, $^{3}J_{HH}$ = 7.8 Hz, $^{4}J_{HH}$ = 2.0 Hz), 7.56-7.52 (m, 3H, arom. CH), 7.34-7.28 (m, 1H, arom. CH), 7.03 (d, 1H, arom. CH, $^{3}J_{HH}$ = 8.1 Hz), 6.98 (t, 1H, arom. CH, $^{3}J_{HH}$ = 7.5 Hz), 5.69 (dd, 1H, CHP, $^{2}J_{PH}$ = 21.3 Hz, $^{3}J_{HH}$ = 10.2 Hz), 4.09-3.99 (m, 2H,

OCH_2CH_3), 3.95-3.83 (m, 1H, OCH_2CH_3), 3.86 (s, 3H, OCH_3), 3.82-3.69 (m, 1H, OCH_2CH_3), 1.18 (t, 3H, $^3J_{HH}$ = 7.1 Hz, OCH_2CH_3), 1.04 (t, 3H, $^3J_{HH}$ = 7.1 Hz, OCH_2CH_3) ppm; **$^{13}C\{^1H\}$ NMR (126 MHz, DMSO-d_6):** δ = 163.08 (d, arom. Cquat ortho of OCH_3, $^2J_{CP}$ = 10.1 Hz), 158.12 (s, arom. Cquat C(Ph)=N), 156.37 (d, arom. Cquat C(NH)=N, $^3J_{CP}$ = 5.7 Hz), 130.69 (s, arom. CH), 129.32 (s, arom. CH), 128.74 (d, arom. CH, $^3J_{CP}$ = 3.5 Hz), 125.17 (s, arom. CH), 124.03 (s, arom. Cquat of C_6H_5), 123.67 (s, arom. Cquat $COCH_3$), 120.34 (s, arom. CH), 110.99 (s, arom. CH), 62.49 (d, OCH_2CH_3, $^2J_{CP}$ = 5.8 Hz), 55.83 (s, OCH_3), 47.17 (d, CHP, $^1J_{CP}$ = 158.3 Hz), 16.24 (d, OCH_2CH_3, $^3J_{CP}$ = 5.4 Hz), 16.01 (d, OCH_2CH_3, $^3J_{CP}$ = 5.4 Hz) ppm; **$^{31}P\{^1H\}$ NMR (121 MHz, DMSO-d_6):** δ = 20.7 (s, P(O)) ppm. IR: ν = 1604 cm^{-1} (C=N). MS (ESI-TOF): m/z = 418.15 $[M + H]^+$, 440.13 $[M + Na]^+$, 456.11 $[M + K]^+$ (expected isotopic profiles). Elemental analysis calcd. (%) for $C_{20}H_{24}O_5N_3P$ (417.40): C 57.55, H 5.80, N 10.07; found C 57.45, H 5.72, N 10.01.

Diethyl[(5-phenyl-1,3,4-oxadiazol-2-ylamino)(4-nitrophenyl) methyl]phosphonate (3c). Yield 76 %. **^1H NMR (300 MHz, DMSO-d_6):** δ = 9.18 (dd, 1H, NH, $^3J_{HH}$ = 9.9 Hz, $^3J_{PH}$ = 3.9 Hz), 8.27 (d, 2H, arom. CH, $^3J_{HH}$ = 8.4 Hz), 7.86-7.82 (m, 4H, arom. CH), 7.55-7.53 (m, 3H, arom. CH), 5.46 (dd, 1H, CHP, $^2J_{PH}$ = 23.1 Hz, $^3J_{HH}$ = 9.9 Hz), 4.12-3.89 (m, 4H, OCH_2CH_3), 1.18 (t, 3H, OCH_2CH_3, $^3J_{HH}$ = 7.1 Hz), 1.12 (t, 3H, OCH_2CH_3, $^3J_{HH}$ = 7.1 Hz) ppm; **$^{13}C\{^1H\}$ NMR (126 MHz, DMSO-d_6):** δ = 162.90 (d, arom. Cquat para of NO_2, $^2J_{CP}$ = 11.1 Hz), 158.50 (s, arom. Cquat C(Ph)=N), 147.16 (d, arom. Cquat C(NH)=N, $^3J_{CP}$ = 2.4 Hz), 143.36 (s, arom. Cquat CNO_2), 130.87 (s, arom. CH), 129.39 (s, arom. CH), 129.33 (s, arom. CH), 125.35 (s, arom. CH), 123.91 (s, arom. Cquat of C_6H_5), 123.39 (s, arom. CH), 63.08 (d, OCH_2CH_3, $^2J_{CP}$ = 22.7 Hz), 63.03 (d, OCH_2CH_3, $^2J_{CP}$ = 22.6 Hz), 54.11 (d, CHP, $^1J_{CP}$ = 152.5 Hz), 16.20 (d, OCH_2CH_3, $^3J_{CP}$ = 15.5 Hz), 16.16 (d, OCH_2CH_3, $^3J_{CP}$ = 15.7 Hz) ppm; **$^{31}P\{^1H\}$ NMR (121 MHz, DMSO-d_6):** δ = 18.8 (s, P(O)) ppm. IR: ν = 1601 cm^{-1} (C=N). MS (ESI-TOF): m/z = 433.13 $[M + H]^+$, 455.11 $[M + Na]^+$, 471.08 $[M + K]^+$ (expected isotopic profiles). Elemental analysis calcd. (%) for $C_{19}H_{21}O_6N_4P$ (432.37): C 52.78, H 4.90, N 12.96; found C 52.84, H 4.94, N 12.91.

General procedure for the synthesis of the ruthenium(II) complexes 4a-c: To a stirred solution (CH_2Cl_2, 15 mL) of diethyl[(5-phenyl-1,3,4-oxadiazol-2-ylamino)(aryl)methyl] phosphonate (**3a-c**) (1.00 mmol) was added a solution of $[RuCl_2(p\text{-cymene})]_2$ (0.306 g, 0.05 mmol) in CH_2Cl_2 (15 mL). After stirring at room temperature for 4 h, the reaction mixture was concentrated to *ca*. 1 mL, upon which *n*-hexane (50 mL) was added. The orange/red precipitate was separated by filtration and dried under vacuum.

Dichloro-{diethyl[(5-phenyl-1,3,4-oxadiazol-2-ylamino)(4-trifluoro-methylphenyl)methyl]phosphonate}(*p*-cymene)ruthenium(II) (4a). Yield 92 %. **^1H NMR (500 MHz, $CDCl_3$):** δ = 8.46 (dd, 1H, NH, $^3J_{HH}$ = 9.0 Hz, $^3J_{PH}$ = 8.0 Hz), 7.73-7.71 (m, 4H, arom. CH), 7.60 (d, 2H, arom. CH, $^3J_{HH}$ = 8.0 Hz), 7.52-7.45 (m, 3H, arom. CH), 5.67 and 5.40 (AA'BB' spin system, 2H, arom. CH of *p*-cymene, $^3J_{HH}$ = 6.0 Hz), 5.65 and 5.38 (AA'BB' spin system, 2H, arom. CH of *p*-cymene, $^3J_{HH}$ = 5.5 Hz), 5.00 (dd, 1H, CHP, $^2J_{PH}$ = 23.0 Hz, $^3J_{HH}$ = 9.0 Hz), 4.28-4.16 (m, 2H, OCH_2CH_3), 4.03-3.91 (m, 2H, OCH_2CH_3), 3.14 (hept, 1H, $CH(CH_3)_2$, $^3J_{HH}$ = 6.7 Hz), 2.33 (s, 3H, CH_3 of *p*-cymene), 1.32 (d, 3H, $CH(CH_3)_2$, $^3J_{HH}$ = 6.7 Hz), 1.31 (d, 3H, $CH(CH_3)_2$, $^3J_{HH}$ = 6.7 Hz), 1.30 (t, 3H, OCH_2CH_3, $^3J_{HH}$ = 6.5 Hz), 1.20 (t, 3H, OCH_2CH_3, $^3J_{HH}$ = 7.0 Hz) ppm; **$^{13}C\{^1H\}$ NMR (126 MHz, $CDCl_3$):** δ = 162.20 (d, arom. Cquat para of CF_3, $^2J_{CP}$ = 11.8 Hz), 156.67 (s, arom. Cquat C(Ph)=N), 138.47 (s, arom. Cquat C(NH)=N), 131.69 (s, arom. CH), 129.26 (s, arom. CH), 128.37 (d, arom. CH, $^3J_{CP}$ = 4.5 Hz), 130.42 (q, arom. Cquat CCF_3, $^2J_{CF}$ = 30.5 Hz), 125.91 (s, arom. CH), 125.67 (s, arom. CH), 124.08 (q, CF_3, $^1J_{CF}$ = 273.2 Hz), 122.98 (s, arom. Cquat of C_6H_5), 103.14 (s, arom. Cquat of *p*-cymene), 98.97 (s, arom. Cquat of *p*-cymene), 83.91 (s, arom. CH of *p*-cymene), 83.82 (s, arom. CH of *p*-cymene), 81.49 (s, arom. CH of *p*-cymene), 81.37 (s, arom. CH of *p*-cymene), 64.72 (d, OCH_2CH_3, $^2J_{CP}$ = 7.1 Hz), 64.33 (d, OCH_2CH_3, $^2J_{CP}$ = 7.3 Hz), 55.68 (d, CHP, $^1J_{CP}$ = 152.5 Hz), 30.78 (s, $CH(CH_3)_2$), 22.45 (s, $CH(CH_3)_2$), 22.41 (s, $CH(CH_3)_2$), 19.00 (s, CH_3 of *p*-cymene), 16.61 (d, OCH_2CH_3, $^3J_{CP}$ = 5.3 Hz), 16.58 (d, OCH_2CH_3, $^3J_{CP}$ = 4.6 Hz) ppm; **$^{31}P\{^1H\}$ NMR (121 MHz, $CDCl_3$):** δ = 15.8 (q, P(O), $^7J_{PF}$ = 2.2 Hz) ppm; **$^{19}F\{^1H\}$ NMR (282 MHz, $CDCl_3$):** δ = -62.68 (d, CF_3, $^7J_{PF}$ = 2.2 Hz) ppm. IR: ν = 1650 cm^{-1} (C=N). MS (ESI-TOF): m/z = 726.10 $[M - Cl]^+$, 784.06 $[M + Na]^+$, 800.04 $[M + K]^+$ (expected isotopic profiles). Elemental analysis calcd. (%) for $C_{30}H_{35}O_4N_3F_3PCl_2Ru$ (761.56): C 47.31, H 4.63, N 5.52; found C 47.24, H 4.55, N 5.48.

Dichloro-{diethyl[(5-phenyl-1,3,4-oxadiazol-2-ylamino)(2-methoxyphenyl)methyl]phosphonate}(*p*-cymene)ruthenium(II) (4b). Yield 81 %. **^1H NMR (500 MHz, $CDCl_3$):** δ = 8.37 (dd, 1H, NH, $^3J_{HH}$ = 6.0 Hz, $^3J_{PH}$ = 9.0 Hz), 7.78 (d, 2H, arom. CH, $^3J_{HH}$ = 6.5 Hz), 7.55 (d, 1H, arom. CH, $^3J_{HH}$ = 7.5 Hz), 7.51-7.47 (m, 3H, arom. CH), 7.21 (t, 1H, arom. CH, $^3J_{HH}$ = 7.7 Hz), 6.94 (t, 1H, arom. CH, $^3J_{HH}$ = 7.5 Hz), 6.84 (d, 1H, arom. CH, $^3J_{HH}$ = 8.0 Hz), 5.63 and 5.36 (AA'BB' spin system, 2H, arom. CH of *p*-cymene, $^3J_{HH}$ = 6.0 Hz), 5.61 and 5.34 (AA'BB' spin system, 2H, arom. CH of *p*-cymene, $^3J_{HH}$ = 6.0 Hz), 5.54 (dd, 1H, CHP, $^2J_{PH}$ = 22.0 Hz, $^3J_{HH}$ = 9.0 Hz), 4.23-4.13 (m, 2H, OCH_2CH_3), 4.07-3.01 (m, 2H, OCH_2CH_3), 3.90 (s, 3H, OCH_3), 3.12 (hept, 1H, $CH(CH_3)_2$, $^3J_{HH}$ = 6.7 Hz), 2.30 (s, 3H, CH_3 of *p*-cymene), 1.29 (d, 3H, $CH(CH_3)_2$, $^3J_{HH}$ = 6.7 Hz), 1.28 (d, 3H, $CH(CH_3)_2$, $^3J_{HH}$ = 6.7 Hz), 1.26 (t, 3H, OCH_2CH_3, $^3J_{HH}$ = 6.5 Hz), 1.24 (t, 3H, OCH_2CH_3, $^3J_{HH}$ = 7.5 Hz) ppm; **$^{13}C\{^1H\}$ NMR (126 MHz, $CDCl_3$):** δ = 162.26 (d, arom. Cquat ortho of OCH_3, $^2J_{CP}$ = 10.6 Hz), 156.77 (d, arom. Cquat C(NH)=N, $^3J_{CP}$ = 5.6 Hz), 156.30 (s, arom. Cquat C(Ph)=N), 131.35 (s, arom. CH), 129.54 (d, arom. CH, $^4J_{CP}$ = 5.1 Hz), 129.51 (d, arom. CH, $^3J_{CP}$ = 7.5 Hz), 129.11 (s, arom. CH), 125.86 (s, arom. CH), 123.38 (s, arom. Cquat $COCH_3$), 122.73 (s, arom. Cquat of C_6H_5), 121.17 (s, arom. CH), 110.63 (s, arom. CH), 103.00 (s, arom. Cquat of *p*-cymene), 98.67 (s, arom. Cquat of *p*-cymene), 83.74 (s, arom. CH of *p*-cymene), 83.72 (s, arom. CH of *p*-cymene), 81.45 (s, arom. CH of *p*-cymene), 81.42 (s, arom. CH of *p*-cymene), 64.05 (d, OCH_2CH_3, $^2J_{CP}$ = 7.1 Hz), 63.81 (d, OCH_2CH_3, $^2J_{CP}$ = 7.3 Hz), 55.96 (s, OCH_3), 49.39 (d, CHP, $^1J_{CP}$ = 158.3 Hz), 30.71 (s, $CH(CH_3)_2$), 22.42 (s, $CH(CH_3)_2$), 22.38 (s, $CH(CH_3)_2$), 18.93 (s, CH_3 of *p*-cymene), 16.63 (d, OCH_2CH_3, $^3J_{CP}$ = 4.4 Hz), 16.60 (d, OCH_2CH_3, $^3J_{CP}$ = 5.0 Hz) ppm; **$^{31}P\{^1H\}$ NMR (121 MHz, $CDCl_3$):** δ = 17.5 (s, P(O)) ppm. IR: ν = 1644 cm^{-1} (C=N). MS (ESI-TOF): m/z = 688.13 $[M - Cl]^+$, 746.09 $[M + Na]^+$, 762.06 $[M + K]^+$ (expected isotopic profiles). Elemental analysis calcd. (%) for $C_{30}H_{38}O_5N_3PCl_2Ru$ (723.59): C 49.80, H 5.29, N 5.81; found C 49.73, H 5.19, N 5.76.

Dichloro-{diethyl[(5-phenyl-1,3,4-oxadiazol-2-ylamino)(4-nitrophenyl)methyl] phosphonate}(*p*-cymene)ruthenium(II) (4c). Yield 82 %. **^1H NMR (500 MHz, $CDCl_3$):** δ = 8.53 (dd, 1H, NH, $^3J_{HH}$ = 8.5 Hz, $^3J_{PH}$ = 8.0 Hz), 8.19 (d, 2H, arom. CH of $O_2NC_6H_4$, $^3J_{HH}$ = 8.0 Hz), 7.81 (d, 2H, arom. CH, $^3J_{HH}$ = 7.5 Hz), 7.72 (d, 2H, arom. CH of $O_2NC_6H_4$, $^3J_{HH}$ = 8.0 Hz), 7.53-7.45 (m, 3H, arom. CH), 5.68 and 5.40

(AA'BB' spin system, 2H, arom. CH of *p*-cymene, $^3J_{HH}$ = 5.5 Hz), 5.65 and 5.39 (AA'BB' spin system, 2H, arom. CH of *p*-cymene, $^3J_{HH}$ = 6.0 Hz), 5.05 (dd, 1H, CHP, $^2J_{PH}$ = 23.5 Hz, $^3J_{HH}$ = 8.5 Hz), 4.28-4.19 (m, 2H, OCH_2CH_3), 4.04-3.95 (m, 2H, OCH_2CH_3), 3.14 (hept, 1H, $CH(CH_3)_2$, $^3J_{HH}$ = 6.7 Hz), 2.33 (s, 3H, CH_3 of *p*-cymene), 1.32 (d, 3H, $CH(CH_3)_2$, $^3J_{HH}$ = 6.7 Hz), 1.31 (d, 3H, $CH(CH_3)_2$, $^3J_{HH}$ = 6.7 Hz), 1.30 (t, 3H, OCH_2CH_3, $^3J_{HH}$ = 7.2 Hz), 1.21 (t, 3H, OCH_2CH_3, $^3J_{HH}$ = 7.0 Hz) ppm; **$^{13}C\{^1H\}$ NMR (126 MHz, $CDCl_3$):** δ = 162.19 (d, arom. Cquat para of NO_2, $^2J_{CP}$ = 11.5 Hz), 156.79 (s, arom. Cquat C(Ph)=N), 147.89 (d, arom. Cquat C(NH)=N, $^3J_{CP}$ = 2.8 Hz), 141.91 (d, arom. Cquat CNO_2, $^5J_{CP}$ = 2.1 Hz), 131.81 (s, arom. CH), 129.31 (s, arom. CH), 128.99 (d, arom. CH, $^3J_{CP}$ = 4.4 Hz), 125.91 (s, arom. CH), 123.88 (s, arom. CH), 122.89 (s, arom. Cquat of C_6H_5), 103.24 (s, arom. Cquat of *p*-cymene), 99.05 (s, arom. Cquat of *p*-cymene), 83.92 (s, arom. CH of *p*-cymene), 83.74 (s, arom. CH of *p*-cymene), 81.50 (s, arom. CH of *p*-cymene), 81.31 (s, arom. CH of *p*-cymene), 64.76 (d, OCH_2CH_3, $^2J_{CP}$ = 7.3 Hz), 64.48 (d, OCH_2CH_3, $^2J_{CP}$ = 7.3 Hz), 55.68 (d, CHP, $^1J_{CP}$ = 151.4 Hz), 30.81 (s, $CH(CH_3)_2$), 22.46 (s, $CH(CH_3)_2$), 22.40 (s, $CH(CH_3)_2$), 18.99 (s, CH_3 of *p*-cymene), 16.61 (d, OCH_2CH_3, $^3J_{CP}$ = 5.0 Hz), 16.58 (d, OCH_2CH_3, $^3J_{CP}$ = 4.4 Hz) ppm; **$^{31}P\{^1H\}$ NMR (121 MHz, $CDCl_3$):** δ = 15.1 (s, P(O)) ppm. IR: ν = 1650 cm^{-1} (C=N). MS (ESI-TOF): m/z = 703.10 $[M - Cl]^+$, 761.06 $[M + Na]^+$, 777.04 $[M + K]^+$ (expected isotopic profiles). Elemental analysis calcd. (%) for $C_{29}H_{35}O_6N_4PCl_2Ru$ (738.56): C 47.16, H 4.78, N 7.59; found C 47.08, H 4.66, N 7.54.

General procedure for the ruthenium-catalyzed reduction of ketones. A 10 mL-Schlenk tube was filled with the ruthenium precursor (1.0 mol %), NaOH (0.25 mol), and ketone (1.0 mmol). ^{i}PrOH (5 mL) was then added. The reaction mixture was stirred at 100°C for 2 h. An aliquot (0.25 mL) of the resulting solution was then passed through a Millipore filter, the solvent was then removed under vacuum and the resulting crude solution was analyzed by ^{1}H NMR spectroscopy.

X-ray Crystal Structure Analysis

Single crystals of **3b** suitable for X-ray analysis were obtained by slow evaporation of a diethyl ether solution of the crude reaction mixture. Crystal data: $C_{20}H_{24}N_3O_5P$, Mr = 417.40 g mol^{-1}, triclinic, space group *P* -1, *a* = 8.8977(11) Å, *b* = 12.5369(14) Å, *c* = 19.5140(20) Å, α = 90.816(4)°, β = 94.235(4)°, γ = 103.384(4)°, *V* = 2110.8(4) $Å^3$, *Z* = 4, *D* = 1.313 g cm^{-3}, μ = 0.166 mm^{-1}, *F*(000) = 880, *T* = 120(2) K. The sample (0.220 x 0.200 x 0.180) was studied on a Bruker PHOTON-III CPAD using Mo-K_α radiation (λ = 0.71073 Å). The data collection ($2\theta_{max}$ = 28.012°, omega scan frames by using 0.7° omega rotation and 30 s per frame, range *hkl*: *h* -11,11 *k* -16,16 *l* -25,25) gave 95,599 reflections. The structure was solved with SHELXT-2014/5,[18] which revealed the non-hydrogen atoms of the molecule. After anisotropic refinement, all of the hydrogen atoms were found with a Fourier difference map. The structure was refined with SHELXL-2014/7[19] by the full-matrix least-square techniques (use of *F* square magnitude; *x*, *y*, *z*, β_{ij} for C, N, O and P atoms; *x*, *y*, *z* in riding mode for H atoms); 538 variables and 8,283 observations with $I > 2.0\ \sigma(I)$; calcd. $w = 1/[\sigma^2(Fo^2) + (0.0942P)^2 + 8.1397P]$ where $P = (Fo^2 + 2Fc^2)/3$, with the resulting R = 0.0823, R_W = 0.2412 and S_W = 1.036, $\Delta\rho < 0.677$ e$Å^{-3}$.

Single crystals of **4a** suitable for X-ray analysis were obtained by slow diffusion of *n*-hexane into a dichloromethane solution of the complex. Crystal data: $C_{30}H_{35}Cl_2F_3N_3O_4PRu$, *Mr* = 761.56 g mol^{-1}, monoclinic, space group $P2_1/n$, *a* = 15.3065(6) Å, b = 13.8547(5) Å, *c* = 15.6247(6) Å, β = 94.198(2)°, *V* = 3304.6(2) $Å^3$, Z = 4, D_x = 1.531 g cm^{-3}, μ = 0.740 mm^{-1}, *F*(000) = 1552, *T* = 120(2) K. The sample (0.080 x 0.100 x 0.100 mm) was studied on a Bruker APEX-II CCD using Mo-K_α radiation (λ = 0.71073 Å). The data collection ($2\vartheta_{max}$ = 27.921°, omega scan frames by using 0.7° omega rotation and 30 s per frame, range *hkl*: *h* -20,20 *k* -18,18 *l* -20,20) gave 98,790 reflections. The structure was solved with SHELXT-2014/5,[18] which revealed the non-hydrogen atoms of the molecule. After anisotropic refinement, all of the hydrogen atoms were found with a Fourier difference map. The structure was refined with SHELXL-2018/3[19] by the full-matrix least-square techniques (use of *F* square magnitude; *x*, *y*, *z*, β_{ij} for C, Cl, F, N, O, P and Ru atoms; *x*, *y*, *z* in riding mode for H atoms); 402 variables and 7,227 observations with $I > 2.0\ \sigma(I)$; calcd. $w = 1/[\sigma2(F_o^2) + (0.0278P)^2 + 3.8006P]$ where $P = (F_o^2 + 2F_c^2)/3$, with the resulting R = 0.0282, R_W = 0.0692 and S_W = 1.048, $\Delta\rho < 0.926$ e$Å^{-3}$.

Single crystals of **4b** suitable for X-ray analysis were obtained by slow diffusion of *n*-hexane into a dichloromethane solution of the complex. Crystal data: $C_{30}H_{38}Cl_2N_3O_5PRu$, *Mr* = 723.57 g mol^{-1}, monoclinic, space group $P2_1/n$, *a* = 11.2342(6) Å, b = 17.0441(10) Å, *c* = 16.4074(8) Å, β = 92.713(2)°, *V* = 3138.1(3) $Å^3$, Z = 4, D_x = 1.532 g cm^{-3}, μ = 0.764 mm^{-1}, *F*(000) = 1488, *T* = 120(2) K. The sample (0.180 x 0.150 x 0.120 mm) was studied on a Bruker PHOTON-III CPAD using Mo-K_α radiation (λ = 0.71073 Å). The data collection ($2\vartheta_{max}$ = 27.932°, omega scan frames by using 0.7° omega rotation and 30 s per frame, range *hkl*: *h* -14,14 *k* -22,22 *l* -21,21) gave 99,843 reflections. The structure was solved with SHELXT-2014/5,[18] which revealed the non-hydrogen atoms of the molecule. After anisotropic refinement, all of the hydrogen atoms were found with a Fourier difference map. The structure was refined with SHELXL-2018/3[19] by the full-matrix least-square techniques (use of *F* square magnitude; *x*, *y*, *z*, β_{ij} for C, Cl, N, O, P and Ru atoms; *x*, *y*, *z* in riding mode for H atoms); 392 variables and 6,696 observations with $I > 2.0\ \sigma(I)$; calcd. $w = 1/[\sigma2(F_o^2) + (0.0252P)^2 + 8.1733P]$ where $P = (F_o^2 + 2F_c^2)/3$, with the resulting R = 0.0417, R_W = 0.0948 and S_W = 1.081, $\Delta\rho < 1.565$ e$Å^{-3}$.

CCDC entries 2076187, 2076185 and 2076186 contains the supplementary crystallographic data, for **3b**, **4a** and **4b** respectively. These data can be obtained free of charge from The Cambridge Crystallographic Data Centre via http://www.ccdc.cam.ac.uk/data_request/cif or by e-mailing data_request@ccdc.cam.ac.uk, or by contacting The Cambridge Crystallographic Data Centre, 12 Union Road, Cambridge CB2 1EZ, UK.

Computational details

All calculations were performed with the Gaussian 09 program,[20] using the functional ωB97XD. Dispersion corrections were included.[21] All atoms were described using the 6-31+G** basis set except the ruthenium atom described by the SDD basis set and associated pseudopotential. The structure was fully optimised and the wavefunction saved. The free enthalpy was extracted from the

frequency calculation performed on this geometry. The weak interactions were studied through the NCI analysis[22] of Gaussian wavefunction. All calculations were performed in the gas phase.

Conflicts of interest

There are no conflicts to declare.

Acknowledgements

We gratefully acknowledges the University of Carthage and the Tunisian Ministry of Higher Education and Scientific Research for the financial support (grant for S. H.).

Notes and references

1 a) J. H. Meyer, P. A. Bartlett, *J. Am. Chem. Soc*., **1998**, *120*, 4600-4609; b) M. Emgenbroich, G. Wulff, *Chem. Eur. J.,* **2003**, *9*, 4106-4117; c) A. K. Bhattacharya, D. S. Raut, K. C. Rana, I. K. Polanki, M. S. Khan, S. Iram, *Eur. J. Med. Chem.,* **2013**, *66*, 146-152; d) A. K. Bhattacharya, D. S. Raut, K. C. Rana, I. K. Polanki, M. S. Khan, S. Iram, *Eur. J. Med. Chem.,* **2013**, *66*, 146-152; e) G.-Y. Yao, M.-Y. Ye, R.-Z. Huang, Y.-J. Li, Y.-M. Pan, Q. Xu, Z.-X. Liao, H.-S. Wang, *Bioorg. Med. Chem. Lett*., **2014**, *24*, 501-507; f) S. A. R. Mulla, M. Y. Pathan, S. P. Gample, D. Sarkar, *RSC Adv*., **2014**, *4*, 7666-7672; g) R. Damiche, S. Chafaa, *J. Mol. Struc*t., **2017**, *1130*, 1009-1017; h) Z.-G. Zeng, N. Liu, F. Lin, X.-Y. Jiang, H.-H. Xu, *Mol. Divers*., **2019**, *23*, 393-401; i) Z. Radai, P*hosphorus Sulfur Silicon Relat. Elem*., **2019**, *194*, 426-437.

1 a) J.-L. Song, J.-G. Mao, *J. Solid State Chem.,* **2005**, *178*, 3514-3521; b) B. Zurowska, B. Boduszek, *Mater. Sci.-Poland*, **2011**, *29*, 105-111; c) B. Zurowska, K. S´lepokura, U. Kalinowska-Lis, B. Boduszek, *Inorg. Chim. Acta*, **2012**, *384*, 143-148.

2 a) M. Juribašić, K. Molčanov, B. Kojić-Prodić, L. Bellotto, M. Kralj, F. Zani, L. Tušek-Božić, *J. Inorg. Biochem*., **2011**, *105*, 867-879; b) B. Zurowska, A. Brzuszkiewicz, B. Boduszek, *J. Mol. Struct.,* **2012**, *1028*, 222-226.

3 B. Zurowska, A. Brzuszkiewicz, B. Boduszek, *Inorganica Chim. Acta,* **2013**, *394*, 159-163.

4 a) G. A. Pinna, G. Murineddu, C. Murruzzu, V. Zuco, F. Zunino, G. Cappelletti, R. Artali, G. Cignarella, L. Solano, S. Villa, *ChemMedChem,* **2009**, *4*, 998-1009; b) P. K. Parikh, H. M. Marvaniya, D. J. Sen, *Int. J. Drug Dev. & Res.,* **2011**, *3*, 248-255; c) K. P. Harish, K. N. Mohana, L. Mallesha, B. N. Prasanna Kumar, *Eur. J. Med. Chem.,* **2013**, *65*, 276-283; d) V. R. Pidugu, N. S. Yarla, S. R. Pedada, A. M. Kalle, A. K. Satya, *Bioog. Med. Chem.,* **2016**, *24*, 5611-5617; e) G. Karabanovich, J. Němeček, L. Valášková, A. Carazo, K. Konečná, J. Stolaříková, A. Hrabálek, O. Pavliš, P. Pávek, K. Vávrová, J. Roh, V. Klimešová, *Eur. J. Med. Chem.,* **2017**, *126*, 369-383; f) N. Parizadeh, E. Alipour, S. Soleymani, R. Zabihollahi, M. R. Aghasadeghi, Z. Hajimahdi, A. Zarghi, *Phosphorus Sulfur Silicon Relat. Elem.,* **2018**, *193*, 225-231; g) B. Liu, R. Li, Y. Li, S. Li, J. Yu, B. Zhao, A. Liao, Y. Wang, Z. Wang, A. Lu, Y. Liu, Q. Wang, *J. Agric. Food Chem.,* **2019**, *67*, 1795-1806; h) N. Takahashi, K. Hayashi, Y. Nakagawa, Y. Furutani, M. Toguchi, Y. Shiozaki-Sato, M. Sudoh, S. Kojima, H. Kakeya, *Bioog. Med. Chem. Lett.,* **2019**, *27*, 470-478; i) A. H. Ananth, N. Manikandan, R. K. Rajan, R. Elancheran, L. K., M. Ramanathan, A. Bhattacharjee, S. Kabilan, *Chem. Biodiversity,* **2020**, *17*, e1900659; j) T. Biftu, D. F. Feng, G.-B. Liang, H. Kuo, X. Qian, E. M. Naylor, V. J. Colandrea, M. R. Candelore, M. A. Cascieri, L. F. Colwell, J. M. J. Forrest, G. J. Hom, D. E. MacIntyre, R. A. Stearns, C. D. Strader, M. J. Wyvratt, M. H. Fisher, A. E. Weber, *Bioog. Med. Chem. Lett.,* **2000**, *10*, 1431-1434.

5 a) M. Du, X.-H. Bu, *Bull. Chem. Soc. Jpn.,* **2009**, *82*, 539-554; b) L. Haiduc, *J. Coord. Chem.,* **2019**, *72*, 2127-2159.

6 a) X. Gong, P. K. Ng, W. K. Chan, *Adv. Mater.* **1998**, *10*, 1337-1340; b) W. K. Chan, P. K. Ng, X. Gong, S. Hou, *Appl. Phys. Lett.,* **1999**, *75*, 3920-3922; c) P. K. Ng, X. Gong, S. H. Chan, L. S. M. Lam, W. K. Chan, *Chem. Eur. J,.* **2001**, *7*, 4358-4367; d) C.-Y. Wong, C.-M. Che, M. C. W. Chan, J. Han, K.-H. Leung, D. L. Phillips, K.-Y. Wong, N. Zhu, *J. Am. Chem. Soc.,* **2005**, *127*, 13997-14007; e) N. J. Lundin, P. J. Walsh, S. L. Howell, A. G. Blackman, K. C. Gordon, *Chem. Eur. J.,* **2008**, *14*, 11573-11583; f) J. Wu, H.-Y. Li, L.-C. Kang, D.-P. Li, Q.-L. Xu, Y.-C. Zhu, Y.-M. Tao, Y.-X. Zheng, J.-L. Zuo, X.-Z. You, *J. Organomet. Chem.,* **2010**, *695*, 2048-2056; g) Y.-J. Liu, Y.-P. Zhang, *Z. Anorg. Allg. Chem.,* **2013**, *639*, 533-537.

7 a) V. J. Catalano, T. J. Craig, *Inorg. Chem.,* **2003**, *42*, 321-334; b) C.-H. Lin, H.-C. Kao, C.-J. Hsu, W.-J. Wang, *J. Chin. Chem. Soc.,* **2010**, *57*, 1167-1171; c) P. Florindo, I. J. Marques, C. D. Nunes, A. C. Fernandes, *J. Organomet. Chem.,* **2014**, *760*, 240-247; d) J. Pazinato, O. M. Cruz, K. P. Naidek, A. R. A. Pires, E. Westphal, H. Gallardo, E. Baubichon-Cortay, M. E. M. Rocha, G. R. Martinez, S. M. B. Winnischofer, A. Di Pietro, H. Winnischofer, *Eur. J. Med. Chem.,* **2018**, *148*, 165-177.

8 a) B. Stefane, F. Pozgan, *Top Curr. Chem.,* **2016**, *374*, article number 18; b) D. A. Hey, R. M. Reich, W. Baratta, F. Kühn, *Coord. Chem. Rev.,* **2018**, *374*, 114-132; c) J. M. Gichumbi, H. B. Friedrich, *J. Organomet. Chem.,* **2018**, *866*, 123-143; d) A. Mannu, A. Grabulosa, S. Baldino, *Catalysts,* **2020**, *10*, 162.

9 P. Niu, J. Kang, X. Tian, L. Song, H. Liu, J. Wu, W. Yu, J. Chang, *J. Org. Chem.,* **2015**, *80*, 1018-1024.

10 a) A. N. Pudovik, *Dokl. Akad. Nauk SSSR,* **1950**, *73*, 499-502; b) A. N. Pudovik, *Dokl. Akad. Nauk SSSR,* **1952**, *83*, 865-868.

11 R. Wan, P. Wang, F. Han, Y. Wang, J. Zhang, *Synth. Commun.,* **2011**, *41*, 864-870.

12 C. Fiore, I. Sovic, S. Lukin, I. Halasz, K. Martina, F. Delogu, P. C. Ricci, A. Porcheddu, O. Shemchuk, D. Braga, J.-L. Pirat, D. Virieux, E. Colacino, *ACS Sustainable Chem. Eng.,* **2020**, *8*, 18889-18902.

13 I. Khan, A. Ibrar, J. Simpson, *CrystEngComm,* **2014**, *16*, 164-174.

14 a) B. Çetinkaya, S. Demir, I. Özdemir, L. Toupet, D. Séméril, C. Bruneau, P. H. Dixneuf, *Chem. Eur. J.,* **2003**, *9*, 2323-2330; b) S. Balaji, M. K. M. Subarkhan, R. Ramesh, H. Wang, D. Séméril, *Organometallics,* **2020**, *39*, 1366-1375; c) S. Saranya, R. Ramesh, D. Séméril, *Organometallics,* **2020**, *39*, 3194-3201.

15 a) D. J. M. Snelders, G. van Koten, R. J. M. Klein Gebbink, *J. Am. Chem. Soc.,* **2009**, *131*, 11407-11416; b) L. Monnereau, D. Séméril, D. Matt, L. Toupet, *Chem. Eur. J.,* **2010**, *16*, 9237-9247.

16 L. Kathuria, N. U. Din Reshi, A. G. Samuelson, *Chem. Eur. J.,* **2020**, *7622-7630*.

17 K. M. Sheldrick, *Acta Cryst.,* **2015**, *A71*, 3-8.

18 K. M. Sheldrick, *Acta Cryst.,* **2015**, *C71*, 3-8.

19 M. J. Frisch, G. W. Trucks, H. B. Schlegel, G. E. Scuseria, M. A. Robb, J. R. Cheeseman, G. Scalmani, V. Barone, B. Mennucci, G. A. Petersson, H. Nakatsuji, M. Caricato, X. Li, H. P. Hratchian, A. F. Izmaylov, J. Bloino, G. Zheng, J. L. Sonnenberg, M. Hada, M. Ehara, K. Toyota, R. Fukuda, J. Hasegawa, M. Ishida, T. Nakajima, Y. Honda, O. Kitao, H. Nakai, T. Vreven, J. A. Montgomery Jr., J. E. Peralta, F. Ogliaro, M. Bearpark, J. J. Heyd, E. Brothers, K. N. Kudin, V. N. Staroverov, R. Kobayashi, J. Normand, K. Raghavachari, A. Rendell, J. C. Burant, S. S. Iyengar, J. Tomasi, M. Cossi, N. Rega, J. M. Millam, M. Klene, J. E. Knox, J. B. Cross, V. Bakken, C. Adamo, J. Jaramillo, R. Gomperts, R. E. Stratmann,

O. Yazyev, A. J. Austin, R. Cammi, C. Pomelli, J. W. Ochterski, R. L. Martin, K. Morokuma, V. G. Zakrzewski, G. A. Voth, P. Salvador, J. J. Dannenberg, S. Dapprich, A. D. Daniels, O. Farkas, J. B. Foresman, J. V. Ortiz, J. Cioslowski, D. J. Fox, *Gaussian 09, Revision D.01, Gaussian Inc., Wallingford CT* **2009**.

20 S. Grimme, J. Antony, S. Ehrlich, H. Krieg, *J. Chem. Phys.,* **2010**, *132*, 154104.

21 J. Contreras-Garcia, E. R. Johnson, S. Keinan, R. Chaudret, J.-P. Piquemal, D. N. Beratan, W. T. Yang, *J. Chem. Theory Comput.,* **2011**, *7*, 625-632.